The Journal of Engineering Research Vol. 7 No. 2 (2010) 10-23

Performance Comparison of Adaptive Estimation Techniques for Power System Small-Signal Stability Assessment

E. A. Feilat

Electrical Power Engineering Department, Hijjawi Faculty of Engineering Technology, Yarmouk University, Irbid, Jordan

Received 13 May 2009; accepted 15 March 2010

مقارنة أداء التقنيات التكيفية في تقييم استقرارية أنظمة القوى الكهربائية

أياد أ. الفيلات

الخلاصة: يهدف البحث الى تقييم استقرارية نظام قوى كهربائي مربوط بالشبكة الكهربائية على نطاق واسع من الاحمال الكهربائية باستخدام مفهوم عزمي التزامن والاخماد. لقد تلك استخدام ثلاث تقنيات خوارزمية (أدالاين، مرشح كالمان، مربع الخطأ الاصغر التعاقبي) لحساب عاملي عزم التزامن والاخماد وذلك برصد استجابة النظام ممثلة بإزاحة وسرعة وعزم عضو الدوران. وقد تمت مقارنة أداء هذه التقنيات من حيث السرعة والدقة وذلك من خلال إجراء عدة دراسات حاسوبية تحاكي أداء النظام الكهربائي على نطاق واسع من الاحمال الكهربائية وقد وجد في هذا البحث أن أداء مربع الخطأ الاصغر التعاقبي هو الافضل حيث انه الاقل تعقيدا من الناحية الحسابية ويحتاج وقت أقل. وبناء عليه فقد تم استخدام هذه التقنية في تقييم استقرارية أنظمة القوى الكهربائية غير المزودة بحواكم استقرارية نظم القوى الكهربائية، كما وقت دراسة فعالية الحواكم الاستقرارية في تحسين الاستقرار الديناميكي على نطاق واسع من الاحمال الكهربائية وذلك بحساب عاملي عزم التزامن والاخماد باستخدام خوارزمية الخطأ الاصغر التعاقبي.

المفردات المفتاحية: أدالاين، مرشح كالمان، مربع الخطأ الاصغر التعاقبي ، الاستقرارية، عزم التزامن والاخماد

Abstract: This paper demonstrates the assessment of the small-signal stability of a single-machine infinite-bus power system under widely varying loading conditions using the concept of synchronizing and damping torques coefficients. The coefficients are calculated from the time responses of the rotor angle, speed, and torque of the synchronous generator. Three adaptive computation algorithms including Kalman filtering, Adaline, and recursive least squares have been compared to estimate the synchronizing and damping torque coefficients. The steady-state performance of the three adaptive techniques is compared with the conventional static least squares technique by conducting computer simulations at different loading conditions. The algorithms are compared to each other in terms of speed of convergence and accuracy. The recursive least squares estimation offers several advantages including significant reduction in computing time and computational complexity. The tendency of an unsupplemented static exciter to degrade the system damping for medium and heavy loading is verified. Consequently, a power system stabilizer whose parameters are adjusted to compensate for variations in the system loading is designed using phase compensation method. The effectiveness of the stabilizer in enhancing the dynamic stability over wide range of operating conditions is verified through the calculation of the synchronizing and damping torque coefficients using recursive least square technique.

Keywords: Adaline, Kalman filter, Recursive least square, Stability, Synchronizing and damping torques

E-mail: afeilat@squ.edu.om
Currently with the Department of Electrical and Computer Engineering, College of Engineering, Sultan Qaboos University, PO Box 33, Al-Khoud, Muscat, Sultanate of Oman

The Journal of Engineering Research Vol. 7 No. 2 (2010) 10-23

1. Introduction

Small -signal stability analysis is concerned in the behavior of power systems under small perturbations. Its main objective is to assess the low-frequency oscillations (LFO) resulting from poorly damped rotor oscillations. The most critical types of these oscillations are the local-mode, which occurs between one machine and the rest of the system, and the interarea-mode oscillations that occurs between interconnected machines (Robers, 2000; Yu, 1983; Abdel-Magid and Swift 1976 and Hsu and Chen 1987). Stability assessment of these oscillations is a vital concern and essential for secure power system operation and control. For secure power system operation, the operators need fast and efficient computational tools to allow online stability assessment. This paper is concerned in stability assessment of local mode oscillations.

In reality, power system operating conditions change with time. These operating conditions affect the stability of the synchronous machine. Therefore, a small-signal stability analysis must be repeatedly conducted in system operation and control to provide estimates of stability indices on basis of the given data that are obtained by either measurements or computer simulation, and provide new estimates as new data are received.

Traditionally, small-signal stability analyses are carried out in frequency domain using modal analysis method. This method implies estimation of the characteristic modes of a linearized model of the system. It requires first load flow analysis, linearization of the power system around the operating point, developing a state-space model of the power system, then computing the eigenvalues, eigenvectors, and participation factors (Hsu and Chen 1987). Although eigenvalue analysis is powerful, however, it is not suitable for online application in power system operation, as it requires significantly large computational efforts. Alternative method based on electromagnetic torque deviation has been developed. Torque deviation can be decomposed into synchronizing and damping torques (Demello and Concordia, 1969; deOliveris 1994 and Alden and Shaltout 1979). The synchronizing and damping torques are usually expressed in terms of the torque coefficients K_s and K_d. These coefficients can be calculated repeatedly and can be used to identify the specific electromechanical mode λ that provides the largest contribution to the LFO. Once the poorly damped or even undamped mode is identified, then the parameters of a conventional power system stabilizer (PSS) can be tuned using conventional phase compensation to enhance the dynamic stability of the power system.

A time-domain method based on least squares (LS) minimization technique has been applied to compute K_s and K_d for a single-machine-infinite-bus (SMIB) system (Alden and Shaltout 1979). The LS technique requires the time responses of the changes in rotor angle $\Delta\delta(t)$, rotor speed $\Delta\omega(t)$, and electromagnetic torque $\Delta T_e(t)$. These responses can be obtained by offline computer simulation or online measured data. The significance of this method is that it permits the calculation of the torque coefficients for a machine of any degree of complexity and takes into consideration the effect of all system parameters and variables without the need for modeling assumption. This method has been extended to multimachine power systems (Shaltout and Feilat, 1992). The variations of K_s and K_d over wide range of loading conditions were related to the movement of the low-frequency electromechanical mode(Alden and |Shaltout, 1979; Shaltout and Feilat, 1992 and Shaltout and Feilat, 1993). The LS static estimation technique, however, is time consuming as it requires monitoring of the entire period of oscillation.

An artificial neural network (ANN) based technique was proposed in (Feilat *et al*. 1997) for online estimation of K_s and K_d. A static back propagation neural network (BPNN) has been used to associate the real and reactive power (P-Q) patterns with K_s and K_d. Although, the BPNN has very good learning ability, but it suffers from some drawbacks such as long offline training and the difficulty in determining the appropriate number of hidden layers and hidden neurons. Genetic algorithm (GA) and particle Swarm optimization (PSO) techniques were used for optimal estimation of K_s and K_d (El-Naggar and Al-Othman, 2004 and Al-Othman and El-Nagger, 2005). Another online approach based on generalized least square (GLS) and robust fitting with bisquare weights has been proposed to estimate the synchronizing and damping torque coefficients (Ghesemi and Cafiizares, 2006). Although the above techniques have demonstrated their effectiveness in accurate estimation of the torque coefficients, however it is believed that their computational burden prevents its real-time implementation.

To avoid the computational burden, alternative methods based on adaptive estimation techniques have been developed. These techniques have the merit of quick stability assessment of the LFO on the basis of data samples obtained by measurements. It can also automatically provide new estimates as new data samples are received.

A Kalman filter (KF), based approach was introduced in (Feilat *et al*. 1999) to overcome the drawbacks of the LS by estimating K_s and K_d recursively. Kalman filter as an estimator is widely known to be optimal

The Journal of Engineering Research Vol. 7 No. 2 (2010) 10-23

under state-space representation. It has been extensively used in numerous applications (Adly *et al.* 1984). However, the computational burden of KF and the requirement of complete prior knowledge of the state-space representation and its parameters make its real-time implementation inefficient. This practical difficulty motivated the development of other adaptive filters like Adaline and recursive least squares (RLS).

An adaptive filter technique was developed in (Feilat 2007) based on least mean squares (LMS) algorithm which is optimal in the least squares sense to track changes in the optimal solution arising as each new data point becomes available. The LMS algorithm is derived from least squares technique using steepest descent rule and implemented using single adaptive linear neural network (Adaline). The Adaline was introduced in (Dash *et al.* 1996) as a powerful harmonics tracking technique. The Adaline is simple both in concept and implementation. However, Adaline suffers from main weaknesses such as slow and generally non-uniform convergence and dependency on initial conditions.

In efforts to overcome the drawbacks of Adaline and KF, another adaptive technique for fast online estimation of K_s and K_d using a recursive least squares (RLS) algorithm is presented in this paper. In general, RLS algorithm was employed extensively in parameter estimation and system identification problems (Haykin 1996 and Clarkson 1993). The main advantage of the RLS over Adaline lays in faster convergence and lower steady-state error properties, which are essential for online application. Moreover, the algorithm is simpler than KF in terms of the knowledge of covariance matrices. Besides, it does not need a dynamic model for time-varying parameters. This coupled with lower computational costs, makes RLS an attractive alternative to KF.

In this paper, the RLS technique is presented for estimating K_s and K_d from data samples of $\Delta\delta(t)$, $\Delta\omega(t)$, and $\Delta Te(t)$ by conducting time-domain simulations over wide range of P-Q loadings using MATLAB. The performance of the RLS technique is compared with the performance of KF and Adaline techniques in terms of convergence and steady-state error. The static LS is used as benchmark for steady-state estimates comparison. Moreover, the calculated values of the torque coefficients are used for calculating the optimum values of the parameters of a lead-lag power system stabilizer (PSS) which is used for enhancing the small-signal stability of the power system under widely varying loading conditions.

2. Overview of Parameter Estimation Techniques

Parameter estimation aims at estimating parameters that are constant along the estimation process. It is necessary that a set of measurements shapes the relation between these measurements and the parameters to be estimated. A discrete linear system can be described as:

$$y(k) = H(k-1)X(k) \tag{1}$$

$$z(k) = y(k) + v(k) \tag{2}$$

where $y(k)$ is the system output at time instant k, $z(k)$ is measured system output, and $v(k)$ is a zero-mean white Gaussian noise term which counts for measurement noise and modeling uncertainties. $H(k)$ and $X(k)$ are the information matrix and the unknown parameter vector, respectively. The parameters in X can either be constant or subject to infrequent jumps.

2.1 Static Least Squares Estimation (LS)

In least square estimation unknown parameters of a linear model are chosen in such a way that the sum of the squares of the difference between measured and the predicted values is a minimum. For a linear system this translates into finding the parameters, using all available measurements, that minimizes the sum of square error function as follows:

$$E(\hat{X}, n) = \frac{1}{2}\sum_{i=1}^{n}\left(z(i) - H\hat{X}\right)^2 \tag{3}$$

Differentiating $E(\hat{X}, n)$ with respect to X and setting the derivative to zero will lead to the well-known closed-form LS solution as follows:

$$\hat{X}(k) = \left[H_k^T H_k\right]^{-1}\left[H_k^T z_k\right] = A^{\dagger} z_k \tag{4}$$

where X is known as the LS estimate of X, and $A^{\dagger}$ is the left pseudo inverse matrix. In online LS parameter estimation one has to recalculate (4) each time when a new measurement becomes available. To circumvent the problem of recalculating (4), a recursive version of the above algorithm has been derived.

2.2 Kalman Filtering Estimation (KF)

Kalman filter is an adaptive least square error filter that provides a recursive solution for estimates. Kalman filter is implemented by writing a state equation for the parameters to be estimated. The standard KF has two stages: time-update (prediction) and measurement-update (correction), respectively, in the form:

$$\hat{X}(k) = \Phi(k-1)\hat{X}(k-1) + w(k-1) \tag{5}$$

$$Z(k) = H(k)\hat{X}(k) + v(k) \tag{6}$$

where $X(k)$ is nx1 parameter estimation vector, $\Phi(k)$ is nxn parameter transition matrix, $Z(k)$ is mx1 measure-

The Journal of Engineering Research Vol. 7 No. 2 (2010) 10-23

ment vector, $H(k)$ is mxn measurement matrix, $w(k)$ and $v(k)$ are zero-mean random signal representing measurement errors. The recursive process starts by assuming an initial estimate of $\hat{X}_-(k)$ and its error covariance $P(k)$. The updated state estimate equation is obtained:

$$\hat{X}_+(k) = \hat{X}_-(k) + K(k)\left(z(k) - H(k)\hat{X}_-(k)\right) \quad (7)$$

An update of the covariance matrix is obtained:

$$P_+(k) = \left(I - K(k)H(k)\right)P_-(k) \quad (8)$$

where the Kalman gain matrix K is defined as:

$$K(k) = P_-(k)H^T(k)\Phi(k)^{-1} \quad (9)$$

where

$$\Phi(k) = \left(H(k)P_-(k)H^T(k) + R(k)\right) \quad (10)$$

Next, a prediction of the states based on optimal estimates and the covariance matrix are obtained:

$$\hat{X}_-(k+1) = \Phi(k)\hat{X}_+(k) \quad (11)$$

$$P_-(k+1) = \Phi(k)P_+(k)\Phi^T(k) + Q(k) \quad (12)$$

where $R(k)$ and $Q(k)$ are the covariance matrices of the error random signals $v(k)$ and $w(k)$, respectively.

2.3 Least Mean Squares Estimation (LMS)

Although (4) bears simple and straight implementation of the LS estimation method, this can carry deficient numerical stability in the event of bad conditioned estimation problem. For solving this deficiency, alternative adaptive iterative techniques were developed to avoid direct inversion of (4) to produce stable solution. The iterative technique consists of an adaptive filter acting on input sequence $X(n) = [x_1, x_2, \ldots, x_n]$ at time k to produce an output $y(n)$. The filter is designed so that the output should approximate a desired or training output $d(n)$. The error $e(n)$ between the desired output and the actual output is used to control the filter weights, hence making the filter data adaptive. A normalized iterative formula for the solution is given by the Widrow-Hoff delta adaptation rule:

$$W(k+1) = W(k) + \frac{\alpha e(k)X(k)}{\lambda + X(k)^T X(k)} \quad (13)$$

where $e(k) = d(k) - y(k)$ is the prediction error, $y(k)$ is the estimated signal magnitude, α is the learning parameter (reduction factor), λ is a suitably chosen small positive constant added to the divisor to avoid division by zero. Equation (13) is known as the normalized least mean squares (NLMS) adaptive filter update. The LMS algorithms are derived from LS algorithm using steepest descent rule. The LMS algorithms are attractive as the update equations is computationally simple, requiring no matrix inversion or other expensive operations. The update equation also indicates the possibility of real-time implementation using Adaline as shown in Fig. 1. The Adaline produces a linear combination of its input vector $X(k) = [x_1, x_2, \ldots, x_n]$ at time k. After, the input vector is multiplied by the weight vector $W(k) = [w_1, w_2, \ldots, w_n]$, the weighed inputs are combined to produce the linear output $y(k) = W(k)^T X(k)$. The weight vector is adjusted by an adaptation rule so that the output from the Adaline algorithm $y(k)$ is close to the desired value $d(k)$. Perfect training is attained when the error is brought to zero. The numerical values of α and λ greatly affects the performance of the Adaline estimation.

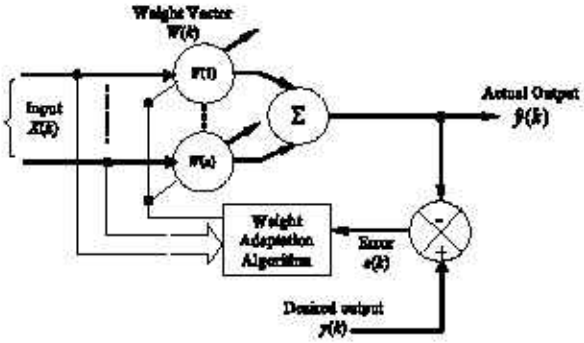

Figure 1. Adaptive LMS estimator architecture (Adaline)

2.4 Recursive Least Squares Estimation (RLS)

For real-time estimation, it is computationally more efficient if the parameter estimates in (4) are updated recursively as new data becomes available online. Such reformulation reduces the computational requirement significantly, making the RLS extremely attractive for on-line parameter estimation application. The recursive estimation algorithm can be written in a number of different equivalent forms (El-Hawary 1989). The following form of the RLS algorithm has many computational advantages. The recursive form is given by:

$$\hat{X}_+(k) = \hat{X}_-(k-1) + K(k)\left(z(k) - H(k)\hat{X}_-(k-1)\right) \quad (14)$$

where the gain matrix $K(k)$ is defined as:

$$K(k) = P_-(k)H(k)\Phi^{-1}(k) \quad (15)$$

where $\Phi(k)$ is defined as:

$$\Phi(k) = \left(1 + H(k)P_-(k)H^T(k)\right) \quad (16)$$

The equivalent of the state error covariance matrix $P(k)$ is given by:

$$P_+(k) = \left(I - K(k)H(k)\right)P_-(k) \quad (17)$$

The Journal of Engineering Research Vol. 7 No. 2 (2010) 10-23

Equation (14) updates the estimates at each step k based on the error between the model output and the predicted output.

The equations for the recursive least squares methods bear many similarities to the Kalman filtering equations. The differences between KF and the RLS method are: in the predictor stage of the KF, a prediction of the state based on the previous optimal estimate is obtained by:

$$\hat{X}_-(k) = \Phi(k-1)X_+(k-1) \tag{18}$$

whereas, in the RLS method, the transition matrix is assumed to be unity and thus:

$$\hat{X}_-(k) = X_+(k) = X(k) \tag{19}$$

In addition, the error covariance matrix is obtained by:

$$P_-(k) = \Phi(k-1)P_+(k-1)\Phi^T(k-1) \tag{20}$$

The RLS algorithm, when applied to parameter estimation, presents two advantages: avoids matrix inversion and needs smaller matrices, which implies less memory storage and computing time.

3. Study Power System

The system considered in this paper is a synchronous machine connected to an infinite bus through two parallel transmission lines as shown in Fig. 2. The machine is equipped with a voltage regulator, a static exciter, and lead a lead-lag PSS. The parameters of the system are given in Appendix A.

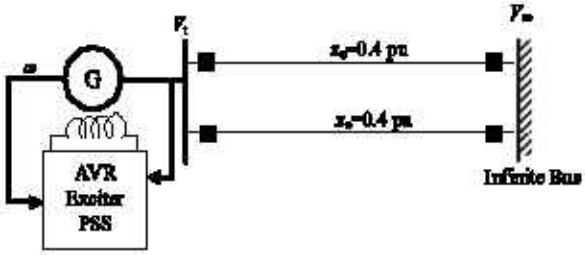

Figure 2. Single-machine infinite-bus (SMIB) system

For small-signal stability analysis, the SMIB system is linearized at a particular operating point to obtain the linearized power system model as follows (Abdel-Magid and Swift 1976):

$$M\frac{d^2\Delta\delta}{dt^2} = \Delta T_m - \Delta T_e \tag{21}$$

$$\Delta T_e = K_1\Delta\delta + K_2\Delta E'_q \tag{22}$$

$$\Delta E'_q = \frac{K_3}{1+sT'_{do}K_3}\Delta E_{fd} - \frac{K_3K_4}{1+sT'_{do}K_3}\Delta\delta \tag{23}$$

$$\Delta V_t = K_5\Delta\delta + K_6\Delta E'_q \tag{24}$$

where T_m and T_e are the mechanical input and electrical output torques of the generator, respectively, M is inertia constant, E_{fd} is the field voltage, and T'_{do} is the open circuit field time constant. The K_1-K_6 constants are the SMIBS constants which, with the exception of K_3 which is only function of the ratio of impedance, are function of the operating real and reactive loading as well as the excitation levels in the generator.

A static type exciter is considered in this study with the voltage state E_{fd}. It is described as:

$$\frac{d\Delta E_{fd}}{dt} = \frac{1}{T_A}\left[K_A(\Delta V_{ref} - \Delta v_t + \Delta u_{PSS}) - \Delta E_{fd}\right] \tag{25}$$

where K_A and T_A are the gain and time constant of the excitation system, respectively. V_{ref} is the reference voltage.

The PSS is modeled using a two-stage phase lead-lag compensator and a washout filter installed in the feedback loop. The input signal is the rotor speed and the output is the PSS signal u_{PSS}.

Figure 3 shows the well-known Phillips-Heffron block diagram of the linearized model of the SMIB system. The interaction between the speed and voltage control equations of the machine is expressed in terms of six constants K1 - K6. The calculations of these constants and variables are given in Appendix B.

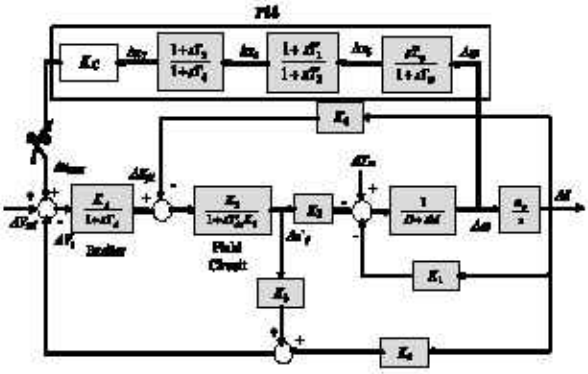

Figure 3. Block-diagram of Phillips-Heffron model

A linearized state-space model in the form of

$$\begin{aligned} dX/dt &= AX + BU \\ Y &= CX + DU \end{aligned} \tag{26}$$

is developed from the Phillips-Heffron block diagram. A fourth-order model with a state vector $X = [\,\Delta\delta\ \Delta\omega\ \Delta E'_q\ \Delta E_{fd}\,]$ is considered for the synchronous generator. The system matrix A is function of the system parameters, which depends on the operating conditions. The perturbation matrix B depends on the system parameters only. The perturbation signal U is either ΔT_m or V_{ref}. The output matrix C relates the desired output signals vector Y to the state variables

The Journal of Engineering Research Vol. 7 No. 2 (2010) 10-23

vector X. The A, B, C, and D matrices of the system are shown in Appendix B.

4. Stability Assessment Using Modal Analysis

When a power system experiences a small disturbance as a result of small changes of loads, the dynamic response of the system states can be described as linear sum of various modes of oscillations (Kalith, 1980):

$$X(t) = \sum_{i=1}^{n} (V_i X_o) e^{\lambda_i t} U_i \tag{27}$$

where λ_i are the distinct eigenvalues of the system matrix A, with a corresponding set of right and left eigenvectors U_i and V_i, respectively. The number of the characteristic modes $e^{\lambda_i t}$ equals to the number of states of the linearized power system model. Real eigenvalues indicate modes, which are *aperiodic*. Complex eigenvalues indicate modes, which are oscillatory. For a complex eigenvalue $\lambda_i = \sigma_i \pm j\omega_i$ the amplitude of the mode varies with as $e^{\sigma_i t}$ and frequency of the oscillation, $f = \omega/2\pi$. Accordingly, by expanding (27), the individual state response $x(t)$ can be computed as:

$$x(t) = \sum_{i=1}^{n} B_i e^{\lambda_i t} = \sum_{i=1}^{n} A_i e^{\sigma_i t} \cos(2\pi f_i t + \phi_i) \tag{28}$$

where A_i, σ_i, f_i, and ϕ_i are the i^{th} mode amplitude, damping factor, frequency, and phase angle, respectively. In SMIB system, the rotor oscillations are dominated by the low-frequency electromechanical mode. The mode is identified by analyzing the right and left eigenvectors in conjunction with the participation factors (Hsu and Chen 1987). Typical time responses of the rotor angle, speed, and electromagnetic torque of a SMIB system following a small pulse increment in the mechanical torque are displayed in Fig. 4.

5. Stability Assessment Using Torque Coefficients

Following a small disturbance, the electromagnetic torque variation is dominated by the low-frequency electromechanical mode. Accordingly, the torque can be decomposed into synchronizing torque component $K_s \Delta\delta(t)$ and a damping torque component $K_d \Delta\omega(t)$ as follows (Demello and Concordia, 1969):

$$\Delta\hat{T}_e(t) = K_s \Delta\delta(t) + K_d \Delta\omega(t) \tag{29}$$

The synchronizing torque is responsible for restoring the rotor angle excursion, while the damping torque damps out the speed deviations. The synchronizing and damping torques are usually expressed in terms of the torque coefficients K_s and K_d. It can be shown that the damping factor σ and the damped frequency ω can be related to K_s and K_d as follows (Hu, 1983):

$$\lambda = \sigma \pm j\omega = -\frac{K_d}{2M} \pm j\sqrt{\frac{\omega_b K_s}{M} - \left(\frac{K_d}{2M}\right)^2} \tag{30}$$

where the damping factor σ and the damped natural frequency ω are related to the damping and synchronizing torque coefficients K_d and K_s, respectively. These coefficients can be calculated repeatedly which makes it suitable for quantitative and qualitative assessment of the absolute as well as relative stability of the power system. In terms of K_s and K_d, both coefficients must be positive for a stable operation of the machine.

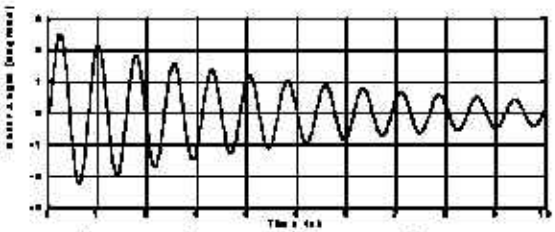

Fig. 4-a Synchronous machine rotor angle response

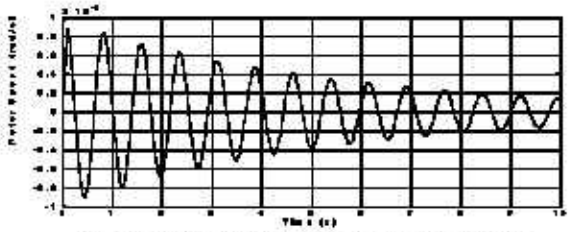

Fig. 4-b Synchronous machine rotor speed response

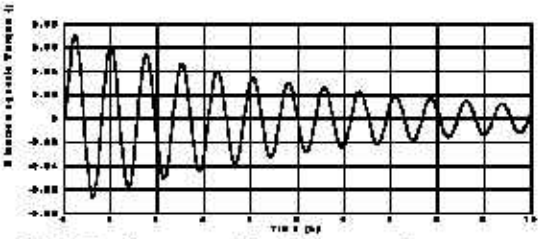

Fig. 4-c Synchronous machine electromagnetic torque response

Figure 4. Synchronous machine time responses

The torque coefficients K_s and K_d can be estimated numerically in time-domain using the time responses $\Delta\delta(t)$, $\Delta\omega(t)$, and $\Delta T_e(t)$. Estimation of K_s and K_d can be described by the discrete state and measurement equations as (Feilat *et al.* 1999):

$$\Delta T_e(k) = HK(k) \tag{31}$$

$$\Delta\hat{T}_e(k) = \Delta T_e(k) + e(k) \tag{32}$$

The Journal of Engineering Research Vol. 7 No. 2 (2010) 10-23

where $H = [\Delta\delta(k)\ \Delta\omega(k)]$ and $X(k) = [K_s\ K_d]^T$ at the time instant k. The estimated parameter vector X is calculated by minimizing the sum of the square error between the electric torque $\Delta T_e(k)$ and the measured torque $\Delta T_e(k)$ using either the static LS technique or any other adaptive technique such as KF, Adaline or RLS technique.

6. Stability Enhancement Using PSS

6.1 PSS Structure and Design

Originally, the LFO problem is tackled by applying PSS, which provides a supplementary excitation control signal to enhance the damping of the poorly damped LFO. The conventional design using a lead-lag compensator as shown in Fig. 3 was investigated on a linearized model of SMIB system because of its simple structure, design and implementation (Rogers, 2000 and Yu 1983). A stabilizing signal derived from generator speed is admitted to the reference input of the automatic voltage regulator (AVR) so that an electrical torque component in phase with speed variation is created to increase system damping. The governing equations of a two-stage lead-lag PSS are given as:

$$(1 + sT_w)\,\Delta x_5 = sT_w\Delta\omega \tag{33}$$

$$(1 + sT_2)\,\Delta x_6 = sT_1\Delta x_5 \tag{34}$$

$$(1 + sT_4)\,\Delta u_{PSS} = K_c\,(1 + sT_3)\,\Delta x_6 \tag{35}$$

PSS typically is designed based on linear control theory using the concept of phase compensation (Yu 1983). The parameters are determined based on a linearized model of the power system around a nominal operating point where they can provide optimum damping performance of LFO. Phase compensation is accomplished by adjusting the PSS parameters (K_C, T_1, T_2, T_3, and T_4) to provide appropriate phase lead to compensate for the phase lags through the generator and AVR-excitation system over a wide frequency range (0.1-2.0 Hz) of LFO such that the PSS provides torque changes $\Delta T_e(t)$ in phase with speed changes $\Delta\omega(t)$. Tuning should be performed when system configuration and operating conditions result in the least damping. Moreover, a good tuning scheme is required to achieve robust performance over a wide range of operating conditions by tuning the PSS parameters according to the damping factor and damped frequency of the poorly damped local mode $\lambda = \sigma \pm j\omega$. In this paper, λ is identified from the torque coefficients K_s and K_d as given by (30).

6.2 PSS Tuning Using Phase Compensation Method

In practice, both the generator and its AVR-exciter exhibit frequency dependent gain and phase characteristics $G_E(s)$. Hence, the PSS transfer function should have appropriate phase-lead circuit to compensate for the phase lag from AVR inputs to the generator electric torque. The steps for designing a PSS can be summarized as follows (Yu 1983):

1. Identify the complex frequency of the local mode, $s = \sigma + j\omega$ using calculated values of the torque coefficients K_s and K_d.
2. Evaluate the transfer function $G_E(s)$ and its phase angle using Phillips-Heffron block diagram with the rotor speed held constant.

$$G_E(s) = \frac{K_4 K_3}{(1+sT_4)(1+sT_{do}'K_3) + K_4 K_3 K_6}\Big|_{s=\sigma+j\omega} = |G_E(s)|\angle\gamma \tag{36}$$

3. Design a phase lead-lag PSS with a phase lead angle $\angle G_c(s) = -\gamma$. For a two-stage lead-lag compensator, the transfer function $G_c(s)$ has the form:

$$G_C = \frac{(1+sT_1)}{(1+sT_2)}\frac{(1+sT_3)}{(1+sT_4)}\Big|_{s=\sigma+j\omega} \tag{37}$$

where T_4=T_2, T_3=T_1 and T_2 is chosen such that $T_1 > T_2$. For fixed values of T_2, T_4 and T_w, the time constant T_1 is calculate, using:

$$T_1 = \frac{\tan\left((\phi-\gamma)/2\right)}{\left(\omega - \sigma\tan\left((\phi-\gamma)/2\right)\right)} \tag{38}$$

where

$$\phi = 2\tan^{-1}\left[\frac{\omega T_2}{1+\sigma T_2}\right] \tag{39}$$

For adequate damping ratio of the new local mode ζ_m, say 0.15, calculate the PSS gain using the root locus method. The gain K_c is given by:

$$K_c = \frac{2\zeta_m\omega_n M}{K_2|G_c|_{s=\sigma+j\omega}|G_E|_{s=\sigma+j\omega}} \tag{40}$$

7. Simulation Results

In this study, the performance of the RLS for the estimation of K_s and K_d is compared with KF and Adaline estimation techniques. The evaluation is carried out by conducting several offline simulation cases on a linearized SMIB system model without PSS using Matlab/Simulink toolbox. The system input is a 0.1 pu mechanical torque pulse (ΔT_m) for 100 ms. The system output vector comprises rotor angle, speed, and electromagnetic torque. A sampling rate of 100 samples per second, over a window size of 10 seconds, is set for all simulation cases.

The Journal of Engineering Research Vol. 7 No. 2 (2010) 10-23

Figures 5 and 6 display the performance of KF, Adaline and RLS in estimating K_s and K_d for a stable light load condition of P_o=0.40 and Q_o=-0.20 pu. It can be seen in Fig.5 the superiority of KF convergence in comparison with Adaline. The Adaline suffers from large oscillations and overshoot, while KF smoothly approaches its final value.

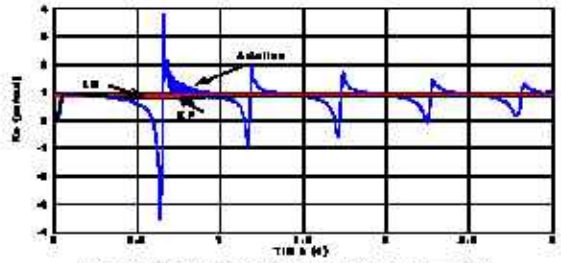

Fig. 5-a Estimation of K_s using Adaline and KF.

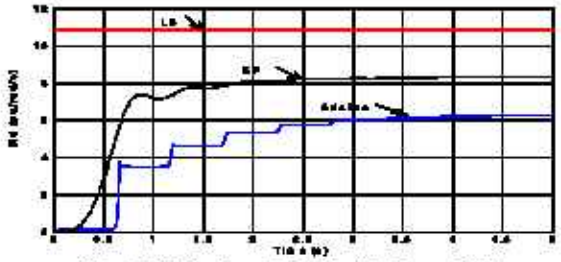

Fig. 5-b Estimation of K_d using Adaline and KF.

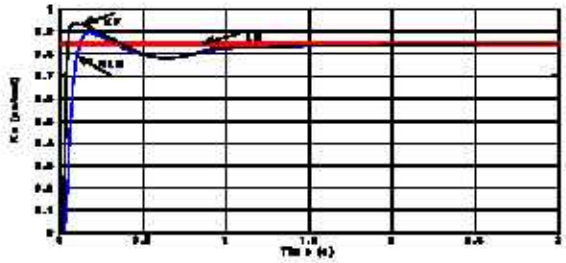

Fig. 6-a Estimation of K_s using RLS and KF.

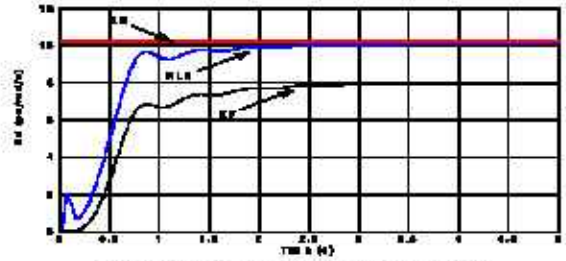

Fig. 6-b Estimation of K_d using RLS and KF.

A comparison of final estimates of K_s and K_d for two operating points are given in Table I. As can be seen, the RLS gives the most accurate estimates in comparison with Adaline or KF.

Likewise, Figs. 7 and 8 shows the performance of KF, Adaline and RLS in estimating K_s and K_d for unstable heavy load condition of P_o=0.80 and Q_o=-0.20 pu. The performance of the RLS in Figs. 7 and 8 relatively outperforms KF convergence behavior and final estimate. It can also be observed that the RLS technique was able to converge to the final estimates of K_s and K_d in one-fifth of the window size.

Table 1. Comparison of final estimates of K_s and K_d

Rotor Mode	Estimates of Torque Coefficients				
	K_i	LS	KF	Adaline	RLS
-0.615 ±j5.797	K_s	0.844	0.844	0.886	0.844
	K_d	10.234	8.149	6.206	10.061
+0.151 ±j6.780	K_s	1.220	1.220	1.220	1.220
	K_d	-3.013	-3.001	-3.018	-3.013

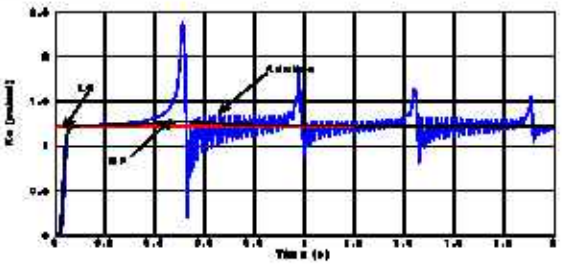

Fig. 7-a Estimation of K_s using Adaline and KF.

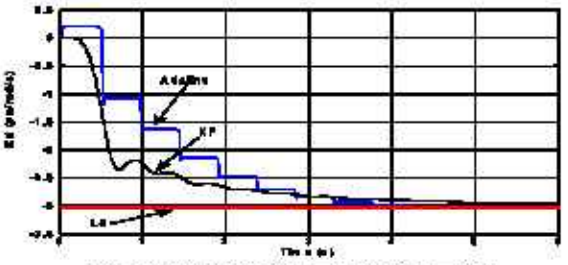

Fig. 7-b Estimation of K_d using Adaline and KF.

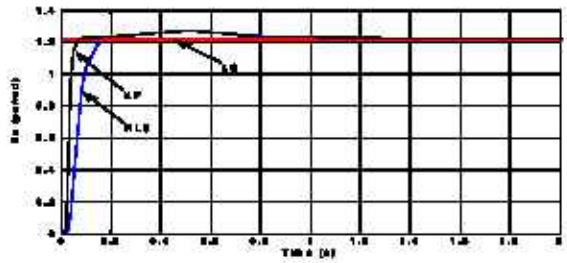

Fig. 8-a Estimation of K_s using RLS and KF.

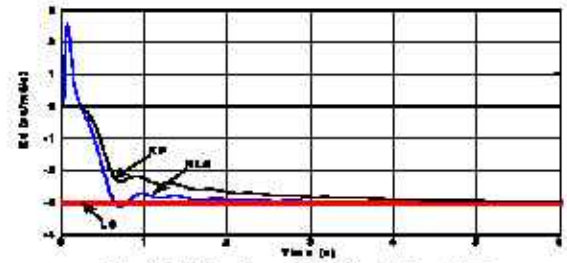

Fig. 8-b Estimation of K_d using RLS and KF.

Variation of the final estimates of the torque coefficients K_s and K_d of the uncompensated SMIBS over a wide range of operating conditions (P_e: 0.1-1.0 pu;

The Journal of Engineering Research Vol. 7 No. 2 (2010) 10-23

Q_e =-0.2-1.0 pu) using RLS technique is depicted in Fig. 9. It is clear that although the synchronizing torque coefficient Ks is positive over that range, however, the machine is unstable for medium and heavy loadings as indicated by negative values of the damping torque coefficient K_d.

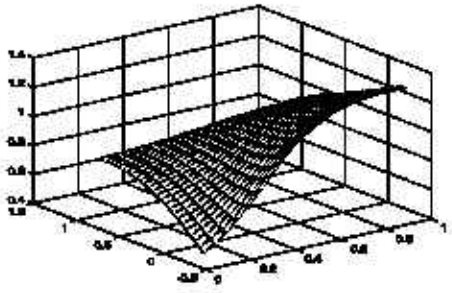

Fig. 9-a Variation of the synchronizing torque coefficient K_s without PSS

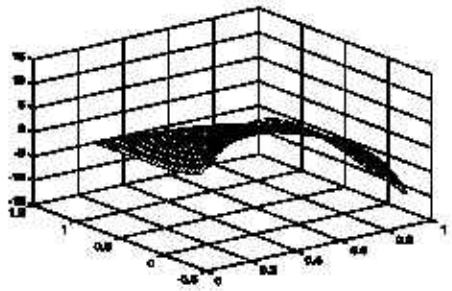

Fig. 9-b Variation of the damping torque coefficient K_d without PSS

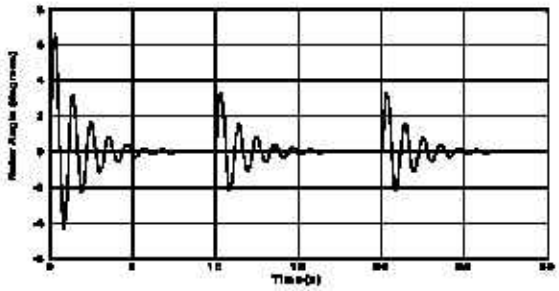

Figure 10. Rotor angle response following sussesive disturbances

The ability of RLS in estimating K_S and K_d following successive disturbances, as shown in Fig. 10, is presented in Fig. 11. The disturbance was created by applying short pulses of mechanical torque for 100 ms. It is evident that RLS is able to obtain accurate estimates of the torque coefficients and responds quickly as new data arrive.

The performance of the RLS technique in estimating K_s and K_d following a loss of a transmission line which yielded an unstable operating point is shown in Figs. 12-13. The load condition is set at P_e = 0.8 pu and Q_e = -0.2 pu and the line is tripped 10 seconds following the first disturbance. Figures 12 and 13 reveal that RLS is capable of tracking large changes in operating condition.

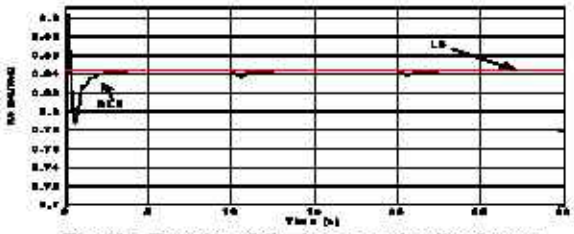

Fig. 11-a K_s tracking following successive disturbances.

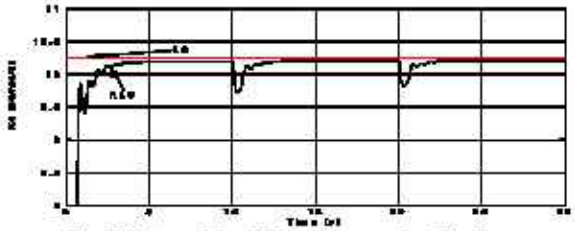

Fig. 11-b K_d tracking following successive disturbances.

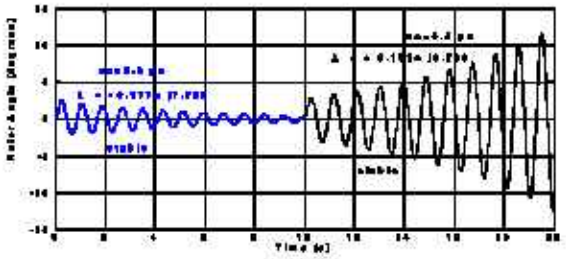

Fig. 12 Rotor angle response following loss of transmission line

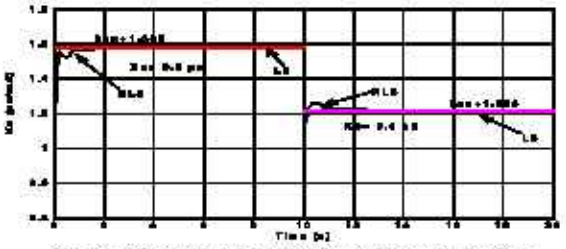

Fig. 13-a K_s tracking following loss of transmission line.

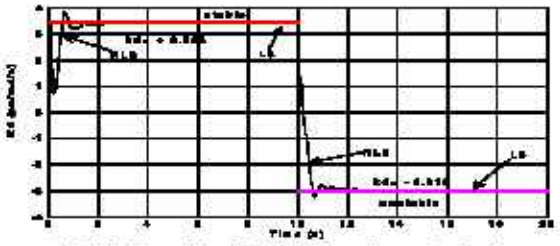

Fig. 13-b K_d tracking following loss of transmission line.

The final estimates of K_s and K_d and the corresponding eigenvalues of the rotor oscillations at the two operating situations are described in Table 2.

Table 2. Estimates of K_s and K_d following loss of line without PSS

Condition	Stable condition	Unstable condition
Parameter	X_e=0.20 (pu)	X_e=0.40 (pu)
$\lambda = \sigma \pm j\omega$	-0.177 ± j7.733	+0.151 ± j6.780
K_s (pu/rad)	1.586	1.220
K_d (pu/rad/s)	3.384	-3.013

The Journal of Engineering Research Vol. 7 No. 2 (2010) 10-23

The effect of variation of the exciter gain K_A on the dynamic performance of the power system is evaluated in terms of the synchronizing and damping torque coefficients K_1 and K_d for two different loading conditions as shown in Fig. 14. It can be seen that high gain values of K_A reduce system stability and produce negative damping torques for certain load conditions. On the other hand, the synchronizing torque coefficient remains relatively unaffected by the large variation of the exciter gain.

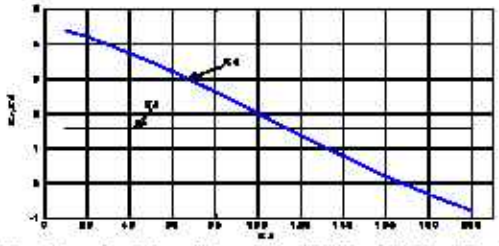

Fig. 14-a Effect of variation of K_A on K_1 and K_d (P_e = 0.8, Q_e=-0.2 pu).

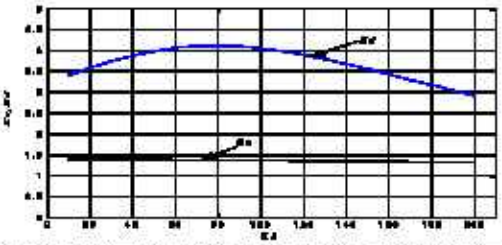

Fig. 14-b Effect of variation of K_A on K_1 and K_d (P_e = 0.8, Q_e=+0.2 pu).

The effect of the PSS on enhancing the small-signal stability of the SMIBS following a loss of a transmission line at a loading condition (P_e =0.8 pu and Q_e = -0.2 pu) is demonstrated in Fig. 15. It can be seen the PSS has effectively improved the dynamic behavior of the SMIBS and stabilized it. The values of the PSS parameters (K_C and T_1) and the corresponding torque coefficients (K_1 and K_d) are illustrated in Table 3.

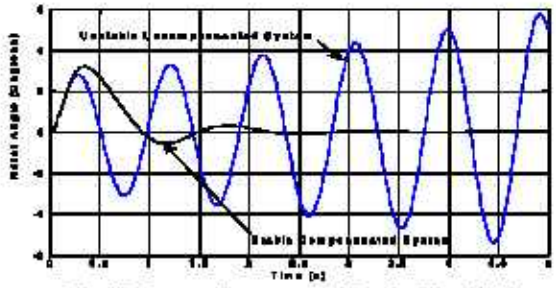

Fig. 15- Rotor angle response with and without PSS

To compute the optimum values of the PSS parameters (K_C and T_1) and the corresponding torque coefficients (K_1 and K_d) over a wide range of loading conditions, a pulse disturbance in the mechanical torque was used to perturb the system from its operating point. Following the method described in section VI, the computed PSS parameters were computed and are plotted in Figs. 16. To obtain optimum values of K_C and T_1 over wide range of loading conditions the damping ratio ξ, and T_2 are set to 0.3 and 0.13, respectively. Moreover, the corresponding synchronizing and damping torque coefficients were calculated using RLS technique and are depicted in Fig. 17. It is clear the tuning PSS with varying load conditions keeps the system stable as indicated by the positive values of the torque coefficients K_1 and K_d.

Table 3. Effect of PSS on small-signal stability

Condition	Unstable condition	Stable condition
Parameter	X_e=0.40 (pu)	X_e=0.40 (pu)
P_e and Q_e	0.8 pu and -0.2 pu	0.8 pu and -0.2 pu
$\lambda = \sigma \pm j\omega$	+0.151 ± *j*6.780	-1.303 ± *j*6.387
K_1 (pu/rad)	1.220	1.213
K_d (pu/rad/s)	-3.013	14.682
K_C	-	0.011
$T_1 = T_3$	-	7.025 *s*
$T_2 = T_4$	-	0.15 *s*

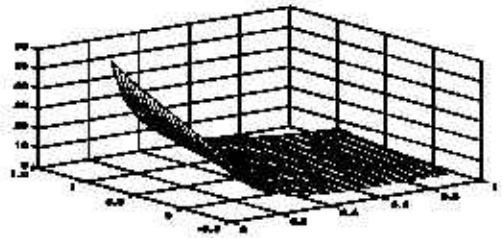

Fig. 16-a Variation of the PSS parameter K_C over wide loadings

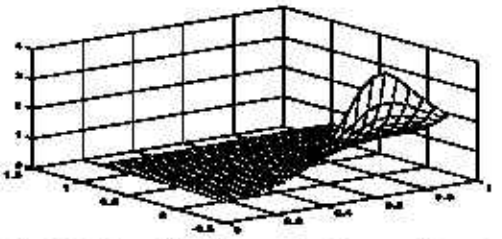

Fig. 16-b Variation of the PSS parameter T_1 over wide loadings

Conclusions

This paper examines the performance of recursive least squares, Kalman filtering, and Adaline estimation techniques for real-time calculation of the synchronizing and damping torque coefficients of a single-machine infinite-bus system.

The accurate estimation of the torque coefficients will help in assessing as well as enhancing the small-signal stability of power systems. The performance of the three adaptive techniques in terms of convergence and steady-state estimate are examined. Compared to Kalman filtering and Adaline, the recursive least squares gives fast and accurate estimates of the torque coefficients. Further, the robustness of the recursive least squares algorithm and its fast convergence reveals that the proposed RLS can be efficiently

employed for real-time dynamic stability assessment of single- and multi-machine power systems by means of the torque coefficients over wide range of operating conditions using digital records of the rotor angle, speed, and electromagnetic torque deviations.

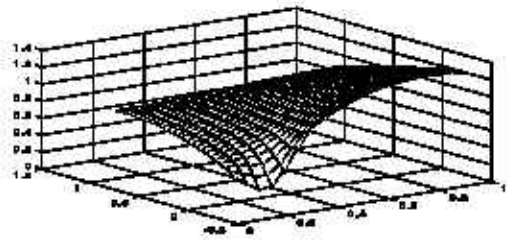

Fig.17-a Variation of the coefficient K_1 with PSS over wide loadings

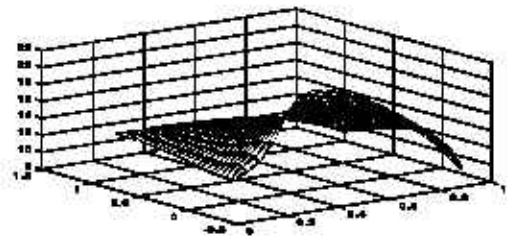

Fig.17-b Variation of the coefficient K_2 with PSS over wide loadings

A power system stabilizer whose parameters are altered to compensate for variations in the system loading is then designed using phase compensation method utilizing the synchronizing and damping torque coefficients. The parameters are optimized offline for a selected set of grid points in the real power and reactive power (P-Q) domain. The effectiveness of the power system stabilizer in enhancing the small-signal stability under widely varying loading conditions is verified through the recalculation of the synchronizing and damping torque coefficients using recursive least-square technique.

References

Abdel-Magid, Y.L. and Swift, G.W., 1976, "Variable Structure Power Stabilizer to Supplement Static-excitation System," IEE Proc. Gen., Trans. & Distr., Pt. C, Vol. 123, No. 7, pp. 697-701.

Adly Girgis, A. and Daniel Hwang, T.L., 1984, "Optimal Estimation of Voltage Phasors and Frequency Deviation Using Linear and Non-linear Kalman Filtering: Theory and Limitations," IEEE Trans. on Power Apparatus and Systems, Vol. PAS-103(10), pp. 2943-2949.

Adly Girgis, A. and Elham Makram., 1988, "Application of Adaptive Kalman Filtering in Fault Classification, Distance Protection, and Fault Location Using Microprocessors," IEEE Trans. Power Systems, Vol. 3(1), pp. 301-309.

Alden, R.T.H. and Shaltout, A.A., 1979, "Analysis of Damping and Synchronizing Torques: Part-I: A General Calculation Method," IEEE Trans. Power Apparatus and Systems, Vol. PAS-98(5), pp. 1696-1700.

AL-Othman, A.K. and EL-Nagger, K.M., 2005, "Estimating Synchronizing and Damping Torque Coefficients Using Particle Swarm Optimization," Proc. 5th IASTED International Conference on Power and Energy Systems, Benalmádena, Spain.

Clarkson, P.M., 1993, "Optimal and Adaptive Signal Processing," CRC Press, Inc.

Dash, P.K., Swain, D.P., Liew, A.C. and Saifur Rahman, 1996, "An Adaptive Linear Combiner for On-line Tracking of Power System Harmonics," IEEE Trans. Power Systems, Vol. PWRS-11(4), pp. 1730-1735.

Demello, F.P. and Concordia, C., 1969, "Concepts of Synchronous Stability as Affected by Excitation Control," IEEE Trans. on Power Apparatus and Systems, Vol. PAS-88(4), pp. 316-329.

deOliveria, S.E.M., 1994, "Synchronizing and Damping Torque Coefficients and Power System Steady-state Stability as Affected by Static VAR Compensation," IEEE Trans. on Power Systems, Vol. PWRS-9(1), pp. 109-119.

El-Hawary, M., 1989, "A Comparison of Recursive Weighted Least Squares Estimation and Kalman Filtering for Source Dynamic Motion Evaluation," Proc. OCEANS'89, pp. 1082-1086.

EL-Naggar, K.M. and AL-Othman, A., 2004, "Genetic Based Algorithms for Estimating Synchronizing and Damping Torque Coefficients," Proc. 4th IASTED International Conference on Power and Energy Systems, Rhodes, Greece, pp. 356-360.

Feilat, E.A., Younan, N. and Grzybowski, S., 1999, "Estimating the Synchronizing and Damping Torque Coefficients Using Kalman Filtering," Electric Power Systems Research, Vol.52(2), pp. 145-149.

Feilat, E.A., 2007, "Fast Estimation of Synchronizing and Damping Torque Coefficients Using an Adaptive Neural Network," Proc. 42nd International Universities Power Engineering Conference, University Of Brighton, Brighton, UK.

Feilat, E.A., Aggoune, E.M., Bettayeb, M. and Al-Duwaish, H., 1997, "On-line Estimation of Synchronizing and Damping Torque Coefficients Using Neural Network Based Approach," Electric Machines and Power Systems, Vol. 25, pp. 993-1007.

Ghasemi, H. and Cañizares, C., 2006, "Damping Torque Estimation and Oscillatory Stability Margin Prediction," Proc. of IEEE PES Summer Meeting, Montreal, Canada.

Haykin, S., 1996, "Adaptive Filter Theory," Prentice Hall, NJ.

The Journal of Engineering Research Vol. 7 No. 2 (2010) 10-23

Hsu, Y.Y. and Chen, C.L., 1987, "Identification of Optimum Location for Stabilizer Applications Using Participation Factors," IEE Proc. Gen., Trans. & Distr., Pt. C, Vol. 134(3), pp. 238-244.

Kailth, T., 1980, " Linear Systems," Prentice-Hall, NJ.

Rogers, G., 2000, "Power System Oscillations," Kluwer Academic Publisher.

Shaltout, A. and Feilat, E.A., 1992, "Damping and Synchronizing Torque Computation in Multimachine Power Systems," IEEE Trans. on Power Systems, Vol. PWRS-7(1), pp. 280-286.

Shaltout, A. and Feilat, E.A., 1993, "Damping and Synchronizing Torque of Closely Coupled generators," Electric Power System Research, Vol. 26(2), pp. 195-202.

Yu, Y.N. 1983 "Electric Power System Dynamics," Academic Press.

The Journal of Engineering Research Vol. 7 No. 2 (2010) 10-23

APPENDIX A

The parameters of the SMIB system are as follows:

Machine Parameters (pu):

$x_d = 1.6, x_q = 1.55, x'_d = 0.32, M = 10.0, T'_{do} = 6.0$ s, $D = 0$

$\omega_b = 120\pi$ rad/s,

Transmission Line (pu):

$r_e = 0.0, x_e = 0.40$ per line

Loading (pu):

$V_{to} = 1.0, P = 0.8, Q = 0.2$.

Exciter/PSS:

$K_A = 50, T_A = 0.05, T_1 = T_3 = 7.03, T_2 = T_4 = 0.15, K_C = 0.01, T_w = 5$

APPENDIX B

For a SMIB system, the following relationships apply with all variables with subscript o are calculated disturbance operating values corresponding to the operating conditions P_o, Q_o, and V_{to}.[5]:

$$i_{qo} = \frac{P_o V_{to}}{\sqrt{(P_o x_q)^2 + (V_{to}^2 + Q_o x_q)^2}} \quad \text{(B-1)}$$

$$v_{do} = i_{qo} x_q \quad \text{(B-2)}$$

$$v_{qo} = \sqrt{V_t^2 - v_{do}^2)} \quad \text{(B-3)}$$

$$i_{do} = \frac{Q_o + x_q i_{qo}^2}{v_{qo}} \quad \text{(B-4)}$$

$$E_{qo} = v_{qo} + i_{do} x_q \quad \text{(B-5)}$$

$$E_o = \sqrt{(v_{do} + x_e i_{qo})^2 + (v_{qo} - x_e i_{do})^2} \quad \text{(B-6)}$$

$$\delta_o = \tan^{-1}\left(\frac{v_{do} + x_e i_{qo}}{v_{qo} - x_e i_{do}}\right) \quad \text{(B-7)}$$

For the case $r_e = 0$, the constants K_1-K_6 are calculated as follows [5]:

$$K_1 = \frac{x_q - x'_d}{x_e + x'_d} i_{qo} E_o \sin\delta_o + \frac{1}{x_e + x_q} E_{qo} E_o \cos\delta_o \quad \text{(B-8)}$$

$$K_2 = \frac{E_o \sin\delta_o}{x_e + x'_d} \quad \text{(B-9)}$$

$$K_3 = \frac{x_e + x'_d}{x_e + x_d} \quad \text{(B10)}$$

$$K_4 = \frac{x_d - x'_d}{x_e + x'_d} E_o \sin\delta_o \quad \text{(B-11)}$$

The Journal of Engineering Research Vol. 7 No. 2 (2010) 10-23

$$K_5 = \frac{X_q}{x_e + x_q}\frac{v_{do}}{V_{to}} E_o \cos\delta_o - \frac{x'_d}{x_e + x'_d}\frac{v_{qo}}{V_{to}} E_o \sin\delta_o \qquad \text{(B-12)}$$

$$K_6 = \frac{x_e}{x_e + x'_d}\frac{v_{qo}}{V_{to}} \qquad \text{(B-13)}$$

The A, B, C, and D matrices of the state-space model (26) are given below:

$$A = \begin{bmatrix} 0 & \omega_o & 0 & 0 & 0 & 0 & 0 \\ -K_1/M & -D/M & -K_2/M & 0 & 0 & 0 & 0 \\ -K_4/T'_{do} & 0 & -1/(T'_{do}K_3) & -1/T'_{do} & 0 & 0 & 0 \\ -K_A K_5/T_A & 0 & -K_A K_6/T_A & -1/T_A & 0 & 0 & K_A/T_A \\ -K_1/M & 0 & -K_2/M & 0 & -1/T_w & 0 & 0 \\ -K_1 T_1/(MT_2) & 0 & -K_2 T_1/(MT_2) & 0 & 1/T_2(1-T_1/T_w) & -1/T_2 & 0 \\ -K_C K_1 T_1 T_5/(MT_2 T_4) & 0 & -K_C K_2 T_1 T_5/(MT_2 T_4) & 0 & K_C T_5/T_2 T_4(1-T_1/T_w) & K_C/T_4(1-T_1/T_2) & -1/T_4 \end{bmatrix}$$

$$B = \begin{bmatrix} 0 & 1/M & 0 & 0 & 1/M & T_1/(MT_2) & K_C T_1 T_5/(MT_2 T_4) \\ 0 & 0 & 0 & K_A/T_A & 0 & 0 & 0 \end{bmatrix}^T$$

$$C = \begin{bmatrix} 1 & 0 & 0 & 0 & 0 & 0 & 0 \\ 0 & 1 & 0 & 0 & 0 & 0 & 0 \\ K_1 & 0 & K_2 & 0 & 0 & 0 & 0 \end{bmatrix}, D = [0]$$